PROCEEDINGS OF ECOS 2023 - THE 36TH INTERNATIONAL CONFERENCE ON
EFFICIENCY, COST, OPTIMIZATION, SIMULATION AND ENVIRONMENTAL IMPACT OF ENERGY SYSTEMS
25-30 JUNE, 2023, LAS PALMAS DE GRAN CANARIA, SPAIN

Exergy assessment of electricity generation via biomass gasification by neural network algorithm.

Gabriel Gomes Vargas[a], Silvio de Oliveira Junior[b]

[a] University of São Paulo, São Paulo, Brazil, gabrielvargas@usp.br
[b] University of São Paulo, São Paulo, Brazil, soj@usp.br

Abstract

The main objective of this study was to develop a prediction model using artificial neural networks (ANNs) and analyze the performance indicators of a green electric energy generation process based on the gasification of Brazilian biomass residues. The recovery of energy from renewable resources is a promising avenue for efficiently delivering valuable products. To achieve this, sugarcane and orange bagasse, residues from the sugarcane harvest, sewage sludge, residues from the corn harvest, coffee residues, eucalyptus residues, and municipal urban waste were used in the proposed process. The Aspen Plus software was used to generate simulation data to predict the energy conversion for each biomass, and a three-layer feed-forward neural network algorithm was employed to build the model. The developed model showed good training and test data accuracy, with an R^2 greater than 0.993. Regarding the performance of the generation plant, the gasification unit provided a maximum of 18.12 MJ/kg of HHV for sewage sludge. Urban and orange waste had the highest cold gas efficiency at 82.21% and 80.66%, respectively. Meanwhile, in the gasification process, sugarcane bagasse and orange residue showed the highest carbon conversion efficiency at 92.88% and 91.17%, respectively. The results indicated that eucalyptus waste gasification could generate more electricity at 12.86 MW. In overall, the study highlights the potential of using ANNs to predict energy conversion and analyze the performance of gasification-based green electric energy generation processes using Brazilian biomass residues.

Keywords:

Biomass gasification, Artificial neural network, Power generation, Exergy analysis.

1. Introduction

Biomass is a significant source of renewable energy that has the potential to reduce fossil fuel dependence and CO_2 emissions. Biofuels have accounted for almost 70% of renewable energy production globally, and biomass was responsible for 25.5% of Brazil's domestic energy supply [1]. Brazil has enormous biomass potential, and biomass wastes could be converted into valuable energy products like hydrogen, ammonia, and electrical energy. This way, energy consumption and greenhouse gas emissions could be reduced, along with waste disposal costs and environmental impact. Brazil has a vast biomass potential, including sugarcane bagasse, orange bagasse, corn, and coffee residues that could be used to produce bioenergy.

Waste-to-energy systems produce electrical and thermal energy using a variety of processes, including combustion, gasification, and power cycles [2]. Sapali and Raibhole [3] examined the combination of air separation and biomass gasification techniques. Because it uses less energy, the low-pressure column's pressure is close to the surrounding atmosphere's pressure of around 1.2 bar, while the high-pressure column operates at about 4 bar. To use less energy than the standard procedure, Wu et al. [4] also modeled a multi-column cryogenic air separation (i.e., high-pressure, low-pressure, and mixed fluid cascade columns) in combination with LNG regasification.

Banerjee et al. [5] also demonstrated a biomass gasification system under various oxygen and vapor ratio circumstances. Five biomass types, including pine, corn, coffee, maple, and straw, were used as fuel for the gasification unit. The fluid bed's gasification temperature was 800°C. Dhanavath et al. [6] have conducted various tests on corn straw, sawdust, and sunflower shells in a fixed bed reactor to study the gasification with stea. The outcomes were contrasted with the process modeling in Aspen Plus. They concluded by reporting that increasing the gasification temperature to 1000ºC produced cold gas with an efficiency of 95% for all inputs. A combined floatation gasification unit and power generation system were described by Lan et al. [7]. They discovered that gradually raising the gasifier's temperature boosted the hydrogen and methane output. In any case, the synthesis gas stream's carbon dioxide content decreased, but the amount of carbon monoxide produced grew considerably.

Artificial neural networks (ANNs) are one of the alternative modeling techniques most utilized at the moment; when compared to other techniques, they may be used to forecast and optimize system outputs in a shorter amount of CPU (Central Processing Unit) time [8]. Although ANN may learn and predict non-linear correlations between the output and input parameters, memorizing the data for training should be avoided [64]. A well-developed ANN model requires careful consideration of the transfer function, training algorithm, and model structure. A powerful and popular analytical technique for the non-linear model is the multi-layer network structure and feed-forward ANN with the backpropagation method [9]. Many studies have adopted ANN models because of their superior effectiveness in predicting the parameters associated

https://doi.org/10.52202/069564-0150

with the gasification process. An ANN model was created by Mikulandric et al. [10] to forecast gasification process parameters, and the findings demonstrated a good correlation with experimental research. The study realized of Serrano et al [11], used an artificial neural network model to predict gas composition and gas yield in a biomass gasification process in a bubbling fluidized bed. The effect of different bed materials was included as a new input, and different network topologies were simulated to determine the best configuration. The developed models were able to predict gas composition and gas yield accurately, indicating that this approach is a powerful tool for efficient design, operation, and control of bubbling fluidized bed gasifiers with different operating conditions, including the effect of bed material.. An ANN model for a combined biomass gasifier-power system was utilized by Safarian et al. [12] to evaluate power output utilizing the features of the biomass and gasifier operation. An ANN model was used by Sozen et al. [13] to look into the energy losses of the heat transformer.

Integrating neural networks and Aspen Plus models present a promising approach to improving the accuracy of power generation predictions. Neural networks can learn complex patterns from operational variables and historical data, making them helpful in predicting generated power. With that in mind, the primary goal of this research was to convert Brazilian waste biomass into renewable energy using waste-to-energy systems, including gasification plants and combined cycles. An Aspen Plus simulation program was used to simulate the bubbling fluidized bed gasifier and combined cycle to achieve this goal. This simulation generated data on the gasification and power generation process, which were used to create a general artificial neural network (ANN) pattern. Some of the significant contributions of this study include proposing a new method for evaluating cycle power generation, implementing machine learning methods on simulation data, and calculating performance indicators as crucial parameters. Finally, the study achieved a new method for generating renewable electricity from waste biomass by integrating these concepts.

2. Methods

2.1. Hypotheses for simulation

In this study, the combustion of volatile and biomass materials is assumed to occur with complete mixing. The Gibbs reactor is used to simplify the simulation, assuming that the gasification reactor is in equilibrium. These assumptions and the software's capabilities allow for accurate predictions of chemical process behaviour, including the physical and chemical properties of mixtures under various operating conditions.

It is important to note that utilizing Aspen Plus for process simulation has limitations. For example, the software cannot account for every factor, such as pressure drops in pipelines or other equipment, and all process-related calculations. However, despite these limitations, Aspen Plus is a powerful and valuable tool for predicting the behaviour of chemical processes, and its use is widespread in the industry.

Also, the following assumptions are considered in the simulation:

1. The system is in a steady state operating condition.
2. Kinetic energy and potential energy changes are neglected.
3. All heat exchangers are assumed to have counter-current flow.
4. Biomass only contains carbon and ash.
5. The volatile materials in the final product of the gasification process are mainly composed of carbon dioxide, carbon monoxide, hydrogen, methane, and water.
6. The pressure drop in the pipelines and other simulation equipment and process-related calculations are ignored.

2.2. Drying and milling process

The flow rate data used in this study were collected through a bibliographic review and data provided by the Basic Sanitation Company of the State of São Paulo [14]. The simulations assumed a constant biomass mass flow rate of 26,400 kg/h, which was kept the same across all simulations, including those performed using neural network analysis.

Figure 1 illustrates the production route that was proposed and analyzed in this study. The process begins with a rotary dryer that removes moisture from the biomass, consuming approximately 15 kWh per wet ton of biomass [15]. The dryer reduces the water content of the biomass to 7% [16]. Following the drying process, the biomass is chipped, and the specific electricity consumption required for the grinding process to obtain 0.5 mm particle diameters [17] was estimated to be approximately 3% of the thermal input of the biomass, based on its lower heating value.

2.3. Waste gasification process

Moving on to the next stage, shown in Fig 1, the gasification unit model was employed using the ultimate and proximate biomass analyses, as illustrated in Table 1. The gasifier model proposed by Battelle Columbus Laboratory (BCL) [18]–[20] was utilized, which is based on an indirect gasification process carried out at atmospheric pressure. This process prevents dilution between the nitrogen present in the produced syngas and the combustion gases. The combustion and gasification processes are carried out separately in a double-column system, with steam serving as the gasification medium.

During the combustion process, a portion of the char produced in the biomass pyrolysis step provides the heat necessary for endothermic drying, pyrolysis, and gasification reactions. Once these reactions are complete, the syngas exits the gasifier, and the produced tar undergoes thermal catalytic cracking. The syngas is then cooled to 400°C and scrubbed with water to remove any impurities that could affect downstream equipment. Finally, the syngas is compressed to 30 bar.

Table 1: Proximate and Ultimate analysis used for different biomass (dry basis) %

Biomass	M_{db}	FC_{db}	VM_{db}	Ash_{db}	C	H	N	S	Cl	O	REF.
Sugar cane bagasse	50.00	14.32	83.54	2.14	46.70	6.02	0.17	0.02	0	44.95	[21]
Sewage sludge	18.40	7.60	64.90	27.50	33.90	6.30	5.88	0.67	0.21	25.50	[22]
Sugar cane straw waste	31.30	12.80	20.60	13.00	49.00	5.60	0.80	0.30	0	44.00	[23]
Coffee waste	8.88	14.48	75.85	0.79	49.33	5.86	0.66	0.04	0	43.24	[24]
Eucalyptus waste	7.73	16.38	74.91	0.98	48.65	6.16	0.28	0	0	44.91	[25]
MSW	49.16	13.94	71.83	14.23	42.04	5.90	0.66	0.10	0	29.87	[26]
Orange bagasse	9.23	13.20	30.60	6.20	46.40	5.54	1.70	0	0	40.15	[27]
Corn waste	60.29	12.62	84.22	0	47.54	6.33	1.32	0.08	0	42.22	[28]

M, moisture content; VM, volatile matter content; FC, fixed carbon content; db, dry basis.

The base of gasification is composed of sequential process pre-treatment (dryer and chipping), pyrolysis, reduction, and combustion processes. Besides, the moisture removal simulation uses a FORTRAN subroutine [18]. To estimate the yield rates of H_2, CO, CO_2, methane, tar, char, and water in the pyrolysis reaction, step one uses empirical correlations reported in the literature as a function of temperature [29]. For this, it is employed an Aspen-embedded Excel spreadsheet.

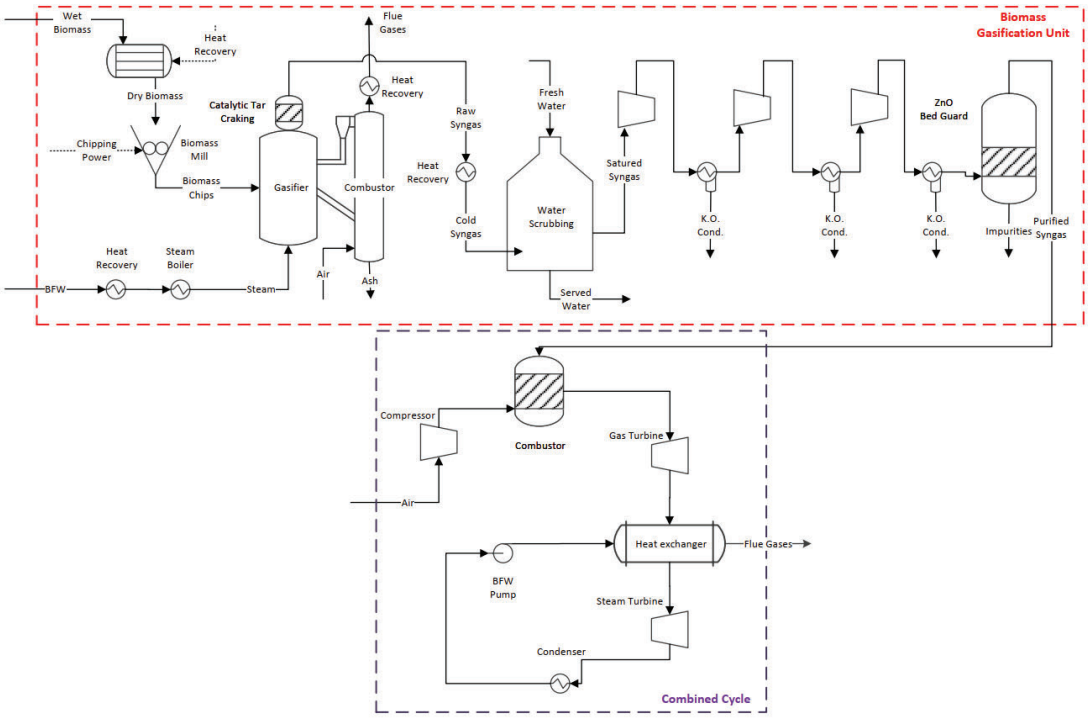

Fig. 1. Superstructure used in the process power conversion of the biomass-based.

2.4. Combined cycle

Figure 1 presents a comprehensive diagram of the combined cycle, depicting the various stages involved. The gas turbine utilized in this system is designed to simulate a Brayton Cycle and is based on the Alstom GT11N2 engine. The specifications for this turbine include mass flow, temperature, and pressure ratio. The steam turbine, on the other hand, operates using a conventional Rankine Cycle, with the simulation parameters being outlined in Table 2. It's worth noting that the same set of assumptions utilized by Silva Ortiz [30] and Medeiros et al [31] have been employed in this study.

To achieve a desired total exit flow rate of 400 kg/s, it is necessary to determine the mass flow rate of air based on the design specifications. The syngas produced during the gasification process serves as the inlet stream in the combustion chamber, where the air and syngas streams are directed to a RStoic reactor for combustion at a prescribed pressure ratio and constant pressure, as presented in Table 2. The gas turbine is designed to maintain the outlet temperature at 526°C. Once the steam temperature is attained, the output gases from the turbine undergo heat exchange with a compressed liquid water stream. Posteriorly, the steam follows to the steam turbine, that operates at an 83% isentropic efficiency and an outlet pressure of 0.1 bar, follows the previously stated pressure and isentropic efficiency assumptions [48, 49]. Ultimately, the water will be cooled in a heat exchanger and pumped back to start a new cycle.

https://doi.org/10.52202/069564-0150

Table 2: Combined cycle variables

Variable	Unit	Value
Compressor pressure ratio	-	15.9:1
Temperature after the gas turbine	°C	526
Pressure after the gas turbine	bar	1
Flue gas temperature	°C	~130
Temperature entering the turbine	°C	510
Pressure entering the turbine	bar	81
Isentropic efficiency of steam turbine	-	83
Pressure after steam turbine	bar	0.1

2.5. Validation

In this study, gasification represents a critical unit operation, given its significant impact on the quality of the final product. To validate the results obtained from the gasification system, It was utilized parameters from Almond shell biomass. Specifically, It was compared our findings with those from a previous study conducted by Marcantonio et al. [32]. and the comparative results are presented in Table 3. The most notable deviation was observed for CO_2, with a discrepancy of approximately 2.13%. However, the deviations for the other substances were relatively minor, with CH_4 showing a deviation of only 0.52%.

Table 3: Gasification results validation.

Parameter	Experimental results [32]	Simulation results	Standard deviation
Proximate analysis (%)			
FC	18.2	18.2	0.00
VM	80.6	80.6	0.00
Moisture	12	12	0.00
Ultimate Analysis (%)			
C	47.9	47.9	0.00
H	6.3	6.3	0.00
O	44.27	44.27	0.00
N	0.32	0.32	0.00
Ash	1.2	1.2	0.00
Volume Fraction (% vol)			
CO	28	29.35	0.95
CO_2	18	14.99	2.13
H_2	44	46.44	1.69
CH_4	10	9.27	0.52

2.6. Artificial neural network

A three-layer feed-forward neural network was employed to model the process of connecting each layer to the one below it. Unlike feedback neural networks, the information in this architecture flows only in one direction, from the input to the output layer. It was assumed that the data gathered accurately represented the system under investigation, a common assumption when working with neural networks. The neural network follows the same structure as described in the work of Cavalcanti et al. [33], with modifications to the inputs and outputs.

To represent the category or categorical-quantitative input variables, one-dimensional zero-arrays were used with a composition value of the component other than zero. This means that nine input neurons were used to represent a proximate and ultimate analysis of biomass, as well as temperature and steam biomass ratio. The ANN design was then expanded to include four neurons in the hidden layer, resulting in 11 input neurons and one output neuron.

To adjust the data, it was used the *NeuralNet package* available in the R software environment [34]. The package trains an ANN by estimating the weights between two neurons in successive layers, which simulate synapses. During training, information is transferred from one neuron to another. The ANN is trained using a sufficiently large dataset to compare its predictions. The training procedure stops when all partial derivatives of the error function E/w concerning the weights are smaller than a specified tolerance, such as 0.01. To compute the error function, it was summed the quadratic errors between observed and predicted values by the ANN.

To mitigate the impact of variable magnitudes on the model predictions, we pre-processed the data using min-max normalization, scaling their values between 0 and 1. The dataset was then randomly split into two subsets: 20% for the

test set, which was solely used to evaluate the ANN's performance, and 80% for the training set, which was used to estimate the ANN weights.

It is important to note that the test data used to evaluate the performance of the ANN must be representative of the same data domain used for training to avoid extrapolations that may result in uncertain predictions. In our case, the ANN included a bias neuron that served as an intercept with sigmoid activation characteristics.

The Resilient Backpropagation with Weight Backtracking (RPROP+) algorithm was used to train the network. Unlike the conventional Backpropagation algorithm, RPROP+ uses a different learning rate for each weight and can be modified during training. This allows for setting a global learning rate suitable for the entire network. RPROP+ only uses the sign of the gradient to update the weights instead of their magnitude, ensuring that the learning rate has an equal impact on the entire network. Weight backtracking refers to erasing the previous weight iteration and adding a smaller value to it in the subsequent step, preventing repeatedly jumping over the minimum. It is important to note that this algorithm is designed to avoid overfitting and improve the model's generalisation ability.

The number of neurons in the hidden layer (NH) was determined to prevent overfitting using the k-fold cross-validation procedure. This technique aims to run the ANN calculations multiple times with different training and test dataset combinations to identify the NH value that results in the lowest mean squared error (MSE) for the test set. This approach helps to ensure that the data used in the analysis are suitable for the ANN model, considering that all data from the articles were employed for training the ANN [35]. The MSE is calculated using Eq. 1.

$$\mathrm{MSE} = \frac{\sum_{i=1}^{a}(P_i - R_i)^2}{a} \tag{1}$$

where for the calculation of MSE; a is the number of data, P_i and R_i are the predicted and real values of the model, respectively.

The topology of the ANN used in this study is shown in Figure 2. The ANN comprises one input layer, one hidden layer with four neurons (NH=4), and one output layer. The inputs to the ANN are gasification temperature (labeled as "temperature" in °C), steam biomass ratio (labeled as "s/b ratio" in %), ultimate analysis of biomass (labeled as "moisture," "volatile material," "fixed carbon," and "ash"), and proximate analysis of biomasses in wt% (labeled as "carbon," "hydrogen," "nitrogen," "sulfur," and "oxygen"). In total, there are 11 input neurons and one output neuron. The ANN topology was generated using the *neuralnet* package available in the R software environment [34]

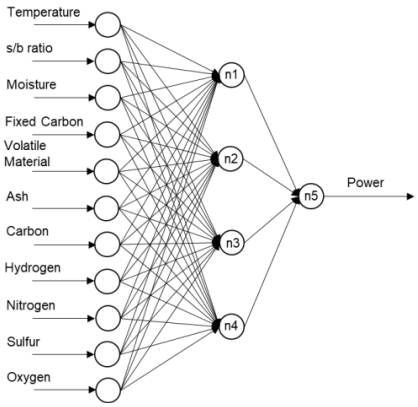

Figure 2. Three-Layer Feedforward Neural Network employed in this work

It is worth noting that none of the covariates directly affect the bias neurons (whose initial value is equal to one) existent to the intercept. The estimated weights calculated during the training phase are also presented in Table 4, where the "From" column indicates the source neuron and the "To" column indicates the destination neuron, as shown in Figure 2.

https://doi.org/10.52202/069564-0150

Table 4: Weights values for each neuron of naeural network

from	to	weight	from	to	weight
Baias	n1	-0.753261712	s/b ratio	n3	0.284048
Temp	n1	0.961899079	Moisture	n3	1.55496
s/b ratio	n1	0.21014481	Fixed Carbon	n3	-0.50962
Moisture	n1	-1.711559624	Volatile Material	n3	-2.5561
Fixed Carbon	n1	-1.538194587	Ash	n3	0.318489
Volatile Material	n1	-0.940108411	Carbon	n3	0.09278
Ash	n1	0.918331711	Hydrogen	n3	0.228348
Carbon	n1	0.207191253	Nitrogen	n3	-0.78659
Hydrogen	n1	-1.386894776	Sulfur	n3	-2.62901
Nitrogen	n1	-0.941899465	Oxygen	n3	-0.8421
Sulfur	n1	-2.042446266	Baias	n4	0.195908
Oxygen	n1	-1.305202095	Temp	n4	-0.2577
Baias	n2	-0.029572741	s/b ratio	n4	0.00124
Temp	n2	0.036312963	Moisture	n4	-1.76798
s/b ratio	n2	-0.483953217	Fixed Carbon	n4	-0.24548
Moisture	n2	3.970044275	Volatile Material	n4	0.110772
Fixed Carbon	n2	0.661251307	Ash	n4	0.157837
Volatile Material	n2	0.106854669	Carbon	n4	-1.10524
Ash	n2	-0.008101265	Hydrogen	n4	-0.6584
Carbon	n2	-0.447942202	Nitrogen	n4	1.105558
Hydrogen	n2	-0.108357221	Sulfur	n4	-0.06553
Nitrogen	n2	1.225302782	Oxygen	n4	0.005014
Sulfur	n2	0.095169143	Baias	n5	1.162488
Oxygen	n2	-0.009455786	n1	n5	1.139094
Baias	n3	-0.602606332	n2	n5	-1.18583
Temp	n3	-0.28335936	n3	n5	0.826087
			n4	n5	0.642381

2.7. Performance indicators

To assess the overall performance of production plants [20], [36], two performance indicators are proposed by Florez-Orrego et al [37] to allow systematic comparisons among the different designed setups: rational and relative exergy efficiencies. The rational efficiency is defined according to Eq. (2), and the relative efficiency by Eq. (3).

$$\eta_{rational} = \frac{B_{useful,output}}{B_{input}} = 1 - \frac{B_{Dest}}{B_{input}} = 1 - \frac{B_{Dest}}{B_{biomass} + W_{input}} \quad (2)$$

$$\eta_{relative} = \frac{B_{consumed,ideal}}{B_{consumed,actual}} = \frac{B_{power}}{B_{biomass} + W_{input}} \quad (3)$$

where, B is the exergy flow rate (kW) and B_{Dest} represents the exergy destroyed rate, while W is the electrical power input to the plant.

The efficiency of a gasifier is typically investigated in terms of two types of efficiency: carbon conversion efficiency and cold gas efficiency. The carbon conversion efficiency (η_{cc}) (Eq. (4)) is defined as the ratio of the reaction carbon ($\boldsymbol{M}_{c_{re}}$) to the feed carbon in the gasifier ($\boldsymbol{M}_{c_{in}}$).

$$\eta_{cc}(\%) = \frac{\boldsymbol{M}_{c_{re}}}{\boldsymbol{M}_{c_{in}}} \quad (4)$$

The higher heating value (HHV) of fuels, including coal, coke, biomass, and municipal wastes, emanates from the heat released from the complete combustion of a unit of mass of fuel at a specific temperature and pressure [38]. Based on HHVs, the cold gas efficiency (η_{cg}) (Eq. (5)) is also expressed as the ratio of the chemical energy of the gas products released from the gasifier to the chemical energy of the input biomass.

$$\eta_{cg}(\%) = \frac{HHV_{syngas} \times M_{syngas}}{HHV_{biomass} \times M_{biomass}} \times 100 \quad (5)$$

The evaluation of each flow's thermodynamic properties and the mass, energy, and exergy balances of each operating unit are evaluated using the Aspen Plus® V8.8 software [39] . Compressors and pumps are modeled using 60% and 80% isentropic efficiencies, respectively. Furthermore, pressure and heat losses are not considered in any process. The ratio of specific chemical exergy (b ^{ch}) to the lower heating value is calculated employing the correlation proposed by [40] for solid fuels with specified mass ratios, Eq. (6)

$$\beta = \frac{b^{ch}}{LHV} = \frac{1.0438 + 0.1882\frac{y_H}{y_C} - 0.2509(1 + 0.7256\frac{y_H}{y_C})}{1 - 0.30350.1882\frac{y_O}{y_C}} \quad (6)$$

where the biomass lower heating value (LHV, MJ/kg) is estimated based on the correlations reported by [41] in Eq. (7)

$$LHV = 349.1y_C + 1178.3y_H + 100.5y_s - 103.4\,y_O - 15.1y_N - 21.5y_{ashes} - 0.0894h_{lv}y_H \quad (7)$$

and y_i are the mass fractions of carbon (C), hydrogen (H), sulfur (S), oxygen (O), nitrogen (N), and ashes (A) in the dry biomass and h_{lv} is the enthalpy of evaporation of water at standard conditions (2442.3 kJ/kg).

Finally, the biomass higher heating value (HHV, MJ/kg) is estimated based on the correlations reported by Parikh et al. [42] in Eq. 8

$$HHV = 0.3536\text{FC} + 0.1559\text{VM} - 0.0078\text{ASH} \quad (8)$$

where FC (%dry basis) is the fixed carbon, and VM is the volatile matter (%dry basis) ASH (%dry basis). The lower heating, high heating, and chemical exergy of biomasses are shown in Table 5.

Table 5: Calculated lower heating value (LHV) and specific chemical exergy value (b^{CH}) for selected materials and fuels streams.

Biomass	HHV (MJ/kg)	LHV (MJ/kg)	b^{CH} (MJ/kg)
Sugar cane bagasse	16.89	15.25	19.50
Sewage sludge	20.28	18.12	16.13
sugar cane waste	16.43	14.89	19.28
Coffee waste	17.06	15.45	19.84
eucalyptus waste	17.19	15.54	21.75
MSW	18.92	17.08	18.32
Orange bagasse	16.79	15.20	20.26
Corn waste	17.87	16.13	19.93

3. Results and discussion

To determine the number of neurons in the hidden layer of the ANN, the data were divided into ten sets using the k-fold cross-validation technique. Each set was then used for training and testing purposes. The mean squared error (MSE) for the testing set was plotted against the number of neurons in the hidden layer (NH), as shown in Fig. 3a. The graph indicates that the MSE value drops to its lowest point at NH = 4 before rising and oscillating, which could be due to overfitting.

Based on the prediction graphs, it was decided that four neurons were sufficient for the ANN hidden layer without compromising the system representation performance. It should be noted that the MSE value for the training set (Fig. 3b) tends to decrease as more neurons and parameters are added to the model, resulting in model overestimation.

https://doi.org/10.52202/069564-0150

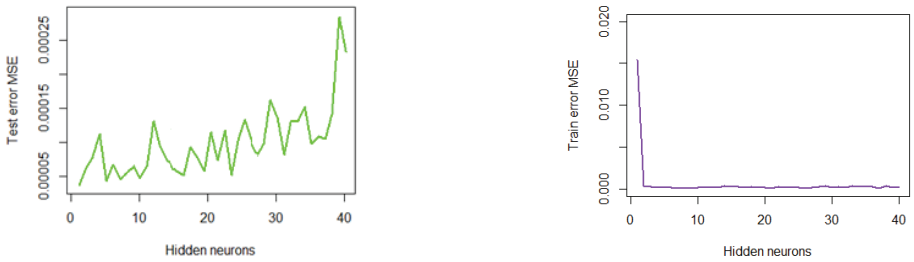

(a) (b)

Figure 3. Mean squared error versus the number of neurons in the hidden layer (a) for the testing set and (b) for the training set.

The training procedure converged after 3309 steps, resulting in an error of 0.04368 for the ANN weights. The accuracy of the ANN model for the training set can be seen in Fig. 4a, which shows an excellent match to the data, as indicated by the high R^2 value of 0.996. The mean square error (MSE) between the observed and projected values was 0.000366. The training set consisted of 80% of the overall dataset, and these data were used to estimate the ANN weights, explaining the good values for R^2 and MSE. Moreover, the residues histogram (Fig. 4b) displayed typical behaviour with an average of roughly zero, further confirming the high agreement between the observed and predicted values.

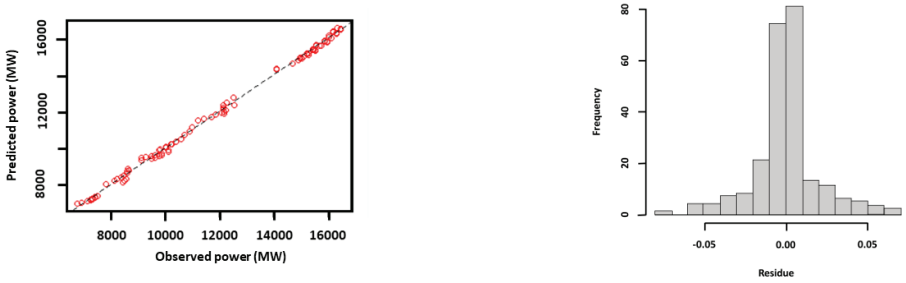

(a) (b)

Figure 4. (a) Comparison between prediction and observed power conversion values for the training set (b) Histogram of residues for the training set.

Fig. 5a demonstrates that the ANN model was validated using the test set. The results indicate that the network can accurately predict data not used in weight estimation, with an R2 value of 0.994 and an MSE of 0.00909. While these metrics are slightly worse than those obtained from the training set, they still reflect a highly credible performance. The corresponding histogram of residuals for this validation, as shown in Fig. 5b, reveals a more significant normal distribution with a less frequent zero-centred average compared to the training set, further corroborating the accuracy of these results.

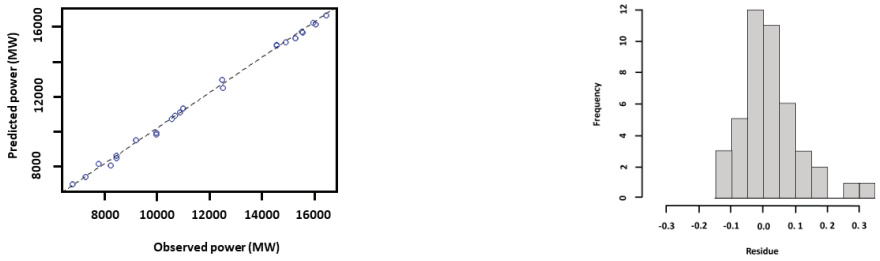

(a) (b)

Figure 5. (a) Comparison between prediction and observed power conversion values for the testing set (b) Histogram of residues for the testing set.

The results presented in Fig. 6 are based on the entire dataset. A residuals histogram displaying a standard shape and an R^2 value of 0.993 and MSE of 0.00172, indicating a good match between predicted and observed values without any noticeable bias in the fit. These performance metrics lie between those obtained from the training and testing sets but are closer to the former, given that the training set contained 80% of the total data and was used to estimate the ANN parameters. Overall, the ANN model exhibits good predictive ability across the entire dataset.

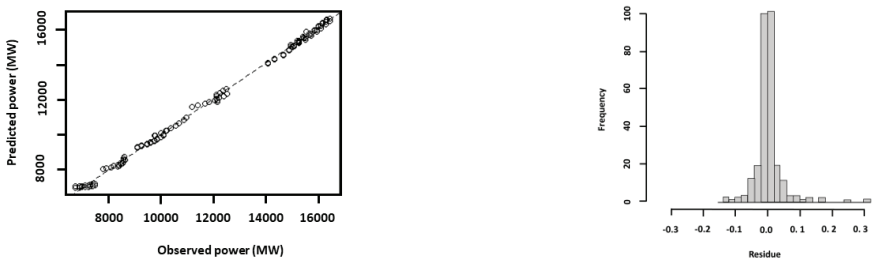

(a) (b)

Figure 6. (a) Comparison between prediction and observed power conversion values for all datasets (b) Histogram of residues for all datasets

To investigate the gasification unit's performance with different fuels, the reactor's initial biomass mass flow rate (26,640kg/h), temperature (850°C), s/b ratio (0.5), and operating pressure were kept constant. The quality of the produced synthesis gas for each fuel was then compared by examining the quantity of its main constituents: H_2, H_2O, CO, and CH_4. Fig. 7 displays the mole fraction of hydrogen and carbon monoxide, the two primary syngas components, in the gasifier's output stream for each fuel. The results reveal that corn waste and sewage sludge produce a high amount of hydrogen but a low mole fraction of carbon monoxide compared to the other biomass fuels.

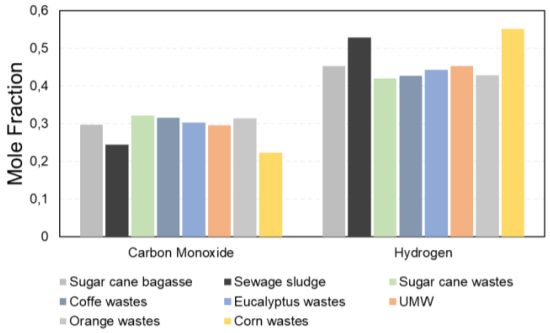

Figure 7 Comparison of syngas quality by the mole fraction of hydrogen and carbon monoxide.

Fig. 8 provides valuable insight into the net power production of different waste materials after the gasification process. The graphic shows that eucalyptus waste, sewage sludge, and sugar cane bagasse have the highest power production potential in the gas turbine section, with 15.86 MW, 15.06 MW, and 14.73 MW, respectively.

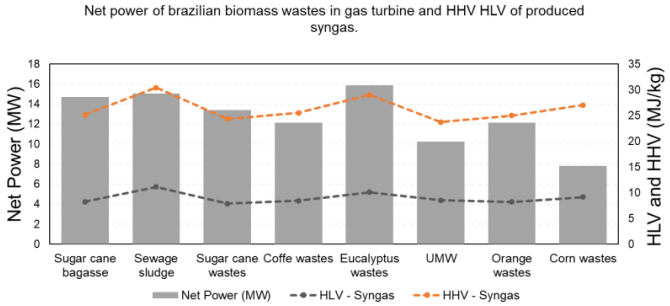

Figure 8. Net power of Brazilian biomass wastes in combined cycle and HHV and LHV of produced syngas

This highlights the importance of utilizing these waste materials as potential energy sources, which can generate significant amounts of power. Additionally, Fig. 8 suggests that the higher the HHV (Higher Heating Value) and LHV (Lower Heating Value) of the produced syngas, the greater the power output from the gas turbine. This underscores the importance of selecting appropriate waste materials for gasification, as those with higher HHV and HLV values can provide greater energy yield and efficiency. Moreover, it is crucial to note that using waste materials for energy production can positively impact the environment by reducing greenhouse gas emissions and mitigating the negative impacts of waste disposal.

Based on the information provided in Fig. 9, It can observe that urban municipal waste has the highest cold gas efficiency (82.21%) among all waste materials studied. This indicates that a significant proportion of the energy content of the waste

https://doi.org/10.52202/069564-0150

material is converted into syngas during the gasification process. On the other hand, sugar cane bagasse exhibits the highest carbon conversion efficiency (92.88%), indicating that most of the carbon content in the waste material is converted into syngas during gasification.

It is important to note that cold gas efficiency (CGE) is affected by various factors, such as the HHV and mass flow rate of waste and syngas. As depicted in Fig. 9, there is a positive correlation between the HHV of syngas and CGE, implying that waste materials with higher HHV values can result in more efficient gasification processes. However, it is also worth mentioning that coffee waste has the lowest cold gas (61.88%) and carbon conversion (72.35%) efficiencies among the waste materials studied. This highlights the need to carefully consider the waste material selection for gasification to ensure optimal efficiency and energy yield.

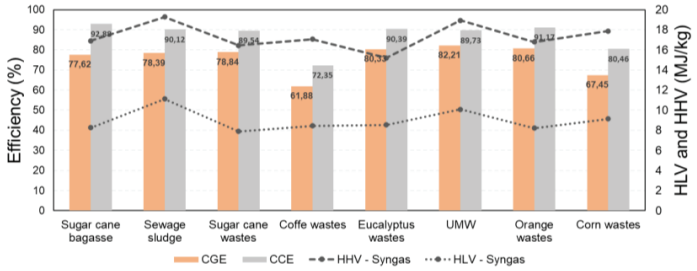

Figure 9: LHV and HHV of syngas, cold gas efficiency (CGE), and carbon conversion efficiency (CCE) of Brazilian biomass wastes in the gasification process.

Figure 10 presents a more detailed view of the destroyed exergy, considering each residual biomasses' leading equipment and processes. Thus, when analyzing these data, it can be noted that the gasifier and the combustor of the combined cycle contribute the largest share of the destruction compared to all biomasses. In addition, it is worth remembering that the syngas' grinding, drying, scrubbing, and compression are also processed internally by the gasification unit. However, compared to the gasification process, they present a small share in the contribution of the exergy destruction of the unit. In addition, it is worth citing the works of Florez-Orrego et al. [18], where the gasification of sugarcane bagasse was studied, and Domingos et al. [19], studying black liquor, obtained similar results.

Observing only the gasifier for the different waste biomasses, the process representing the highest exergy destruction was via RMU, with 68.79%, followed by coffee waste and orange bagasse, with 67.53% and 65.78%, respectively. On the other hand, gasification via sugarcane bagasse had the lowest exergy destruction rate, approximately 58.61%. Also, the combustion process of the combined cycle corresponds to a variation of 22.95% to 30.63% of the exergy destroyed by the entire power conversion process. In other words, exergy destruction in the gasifier is caused by the reactions that decompose the large biomolecules into smaller gas molecules presenting the most considerable exergy destruction compared with combustor burning only syngas.Another essential point to be highlighted is the compression systems, which present intermediate values of exergy destruction. These systems are divided into 3 parts: compression of syngas typical to all conversion plants, air compression of the gas cycle, and pump for the Rankine cycle. The highest proportion of exergy destruction was located in the sewage sludge (2.78%). This happened because the flow rate of syngas after the gasifier is the biggest one compared with other biomasses.

A way to help reduce the amount of exergy destroyed in biomass-based production plants is to employ better technologies to remove the bagasse moisture, hot catalytic cleaning of the syngas, and increase gasifier pressure [43].

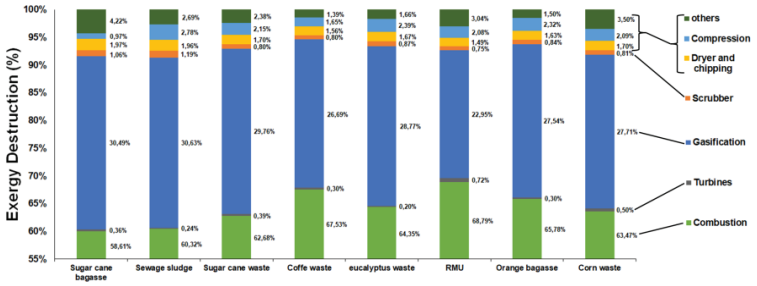

Figure 10: Exergy destroyed by equipment or conversion processes for different biomass waste selected types.

Fig. 11 presents the calculated plantwide efficiencies for different waste materials, revealing that the relative exergy efficiencies ranged from 24.42% for sugar cane straw waste to 42.57% for sugar cane bagasse. Similarly, the rational exergy efficiencies ranged from 23.71% for coffee waste to 39.09% for sugar cane bagasse. These results highlight the significant variability in the energy efficiency of different waste materials. However, it is worth noting that the performance of different biomasses was impaired, likely due to differences in the proximate and ultimate analysis of the waste materials.

Factors such as moisture content and volatile materials can significantly affect the gasification process, leading to variations in energy efficiency. Therefore, it is essential to thoroughly analyse the waste materials before selecting them for gasification to ensure optimal performance and energy yield. By understanding the composition of the waste materials strategies can be developed to optimize the gasification process and improve the energy efficiency of the overall plant.

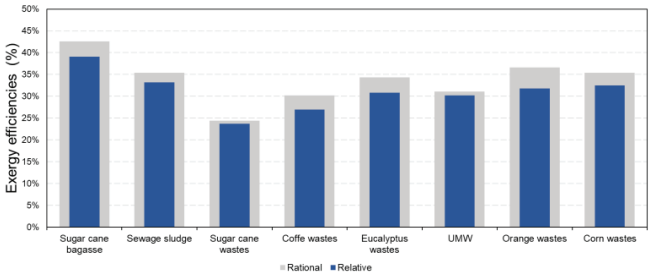

Figure 11. Comparison between the exergy efficiencies of conversion processes for different types of selected biomass.

4. Conclusions

The current research aimed to develop a predictive model using artificial neural networks (ANNs) to analyze the performance indicators of a green electric energy generation process based on the gasification of Brazilian biomass residues. The results indicated that the highest cold gas and carbon conversion efficiencies were achieved using urban municipal waste and sugar cane bagasse with 82.1% and 92.89%, respectively. On the other hand, coffee waste had a relatively low carbon conversion efficiency of about 72.35%, with cold gas efficiency of 61.88%. Eucalyptus waste was found to have the highest renewable power capacity, with 12.86 MW. The relative and rational exergy efficiencies were determined for different waste types, ranging from 24.42% to 42.57% for sugar cane straw waste and sugar cane bagasse, respectively, and from 23.71% to 39.09% for coffee waste and sugar cane bagasse. Furthermore, the study demonstrated the effective use of environmental resources by mapping the exergy destruction reaction to produce a clean and valuable energy source. The study's findings provide important insights into the sustainable utilization of environmental resources by mapping exergy destruction reactions for producing a clean and valuable energy source. These outcomes can be used to guide future research and improve the performance of similar models. However, further studies are necessary to enhance the robustness of ANN models in predicting power generation. More research should be reported in the literature to develop more reliable models. It is worth noting that the ANN model developed in this study exhibited high accuracy in predicting power generation, with R^2 values greater than 0.993 for both training and test datasets. Finally, using neural networks and Aspen Plus models provides a viable solution to improve power generation predictions and reduce computational costs. Applying these methods in this study demonstrates the potential of waste-to-energy systems to generate renewable electricity from waste biomass, promoting a more sustainable energy future.

Acknowledgements

This study was financed in part by the Coordenação de Aperfeiçoamento de Pessoal de Nível Superior - Brasil (CAPES) - Finance Code 001. The first author acknowledges CAPES for his PhD grant. The second author acknowledges CNPq (Brazilian National Council for Scientific and Technological Development) for grant 306484/2020-0.

References

[1] D. Thraen and kay Shaubach, “Global Wood Pellet Industry and Trade Study 2017,” *IEA Bioenergia*, 2017.

[2] W. Foster *et al.*, “Waste-to-energy conversion technologies in the UK: Processes and barriers – A review,” *Renew. Sustain. Energy Rev.*, vol. 135, p. 110226, Jan. 2021, doi: 10.1016/J.RSER.2020.110226.

[3] R. V. Sapali S, “Exergy analysis of cryogenic air separation unit integrated with biomass gasifier.,” *Congr. Eng. Comput. Sci.*, vol. 2, 2013.

[4] Y. Wu, Y. Xiang, L. Cai, H. Liu, and Y. Liang, “Optimization of a novel cryogenic air separation process based on cold energy recovery of LNG with exergoeconomic analysis,” *J. Clean. Prod.*, vol. 275, p. 123027, Dec. 2020, doi: 10.1016/J.JCLEPRO.2020.123027.

[5] S. Banerjee, J. A. Tiarks, and S. C. Kong, “Modeling biomass gasification system using multistep kinetics under various oxygen–steam conditions,” *Environ. Prog. Sustain. Energy*, vol. 34, no. 4, pp. 1148–1155, Jul. 2015, doi: 10.1002/EP.12109.

[6] K. N. Dhanavath, K. Shah, S. K. Bhargava, S. Bankupalli, and R. Parthasarathy, “Oxygen–steam gasification of karanja press seed cake: Fixed bed experiments, ASPEN Plus process model development and benchmarking with saw dust, rice husk and sunflower husk,” *J. Environ. Chem. Eng.*, vol. 6, no. 2, pp. 3061–3069, Apr. 2018, doi: 10.1016/J.JECE.2018.04.046.

[7] W. Lan, G. Chen, X. Zhu, X. Wang, C. Liu, and B. Xu, “Biomass gasification-gas turbine combustion for power generation system model based on ASPEN PLUS,” *Sci. Total Environ.*, vol. 628–629, pp. 1278–1286, Jul. 2018, doi: 10.1016/J.SCITOTENV.2018.02.159.

[8] M. H. Sahraei, M. A. Duchesne, P. G. Boisvert, R. W. Hughes, and L. A. Ricardez-Sandoval, “Reduced-Order Modeling of a Commercial-Scale Gasifier Using a Multielement Injector Feed System,” *Ind. Eng. Chem. Res.*, vol.

https://doi.org/10.52202/069564-0150

56, no. 25, pp. 7285–7300, Jun. 2017, doi: 10.1021/ACS.IECR.7B00693/ASSET/IMAGES/MEDIUM/IE-2017-00693B_0014.GIF.

[9] H. Wang, D. Chaffart, and L. A. Ricardez-Sandoval, “Modelling and optimization of a pilot-scale entrained-flow gasifier using artificial neural networks,” *Energy*, vol. 188, p. 116076, Dec. 2019, doi: 10.1016/J.ENERGY.2019.116076.

[10] R. Mikulandrić, D. Lončar, D. Böhning, R. Böhme, and M. Beckmann, “Artificial neural network modelling approach for a biomass gasification process in fixed bed gasifiers,” *Energy Convers. Manag.*, vol. 87, pp. 1210–1223, Nov. 2014, doi: 10.1016/J.ENCONMAN.2014.03.036.

[11] D. Serrano, I. Golpour, and S. Sánchez-Delgado, “Predicting the effect of bed materials in bubbling fluidized bed gasification using artificial neural networks (ANNs) modeling approach,” *Fuel*, vol. 266, p. 117021, Apr. 2020, doi: 10.1016/J.FUEL.2020.117021.

[12] S. Safarian, S. M. Ebrahimi Saryazdi, R. Unnthorsson, and C. Richter, “Artificial neural network integrated with thermodynamic equilibrium modeling of downdraft biomass gasification-power production plant,” *Energy*, vol. 213, p. 118800, Dec. 2020, doi: 10.1016/J.ENERGY.2020.118800.

[13] A. Sözen and E. Arcaklioğlu, “Exergy analysis of an ejector-absorption heat transformer using artificial neural network approach,” *Appl. Therm. Eng.*, vol. 27, no. 2–3, pp. 481–491, Feb. 2007, doi: 10.1016/J.APPLTHERMALENG.2006.06.012.

[14] SABESP, “State Basic Sanitation Company From Sao Paulo (in portugese).” São Paulo, [Online]. Available: www.sabesp.gov.br.

[15] A. Sues Caula, “Are European bioenergy targets achievable? : an evaluation based on thermoeconomic and environmental indicators,” Technische Universiteit Eindhoven, 2011.

[16] P. Basu, “Biomass Gasification and Pyrolysis,” *Biomass Gasif. Pyrolysis*, 2010, doi: 10.1016/C2009-0-20099-7.

[17] P. C. A. Bergman *et al.*, “Torrefaction for entrained-flow gasification of biomass Revisions A B Made by,” Accessed: Aug. 11, 2021. [Online]. Available: www.ecn.nl/biomass.

[18] D. Flórez-Orrego, F. Maréchal, and S. de Oliveira Junior, “Comparative exergy and economic assessment of fossil and biomass-based routes for ammonia production,” *Energy Convers. Manag.*, vol. 194, pp. 22–36, 2019, doi: https://doi.org/10.1016/j.enconman.2019.04.072.

[19] M. E. G. R. Domingos, D. Flórez-Orrego, M. T. dos Santos, H. I. Velásquez, and S. de Oliveira, “Exergy and environmental analysis of black liquor upgrading gasification in an integrated kraft pulp and ammonia production plant,” *Int. J. Exergy*, vol. 35, no. 1, pp. 35–65, 2021, doi: 10.1504/IJEX.2021.115083.

[20] R. Nakashima, D. Flórez-Orrego, and S. de Oliveira Junior, “Integrated anaerobic digestion and gasification processes for upgrade of ethanol biorefinery residues,” *J. Power Technol.*, vol. 99, no. 2, pp. 104–114, 2019.

[21] Y. C. Ardila, J. E. J. Figueroa, B. H. Lunelli, R. M. Filho, and M. R. W. Maciel, “Syngas production from sugar cane bagasse in a circulating fluidized bed gasifier using Aspen Plus™: Modelling and Simulation,” *Comput. Aided Chem. Eng.*, vol. 30, pp. 1093–1097, Jan. 2012, doi: 10.1016/B978-0-444-59520-1.50077-4.

[22] M. P. Languer *et al.*, “Insights into pyrolysis characteristics of Brazilian high-ash sewage sludges using thermogravimetric analysis and bench-scale experiments with GC-MS to evaluate their bioenergy potential,” *Biomass and Bioenergy*, vol. 138, p. 105614, Jul. 2020, doi: 10.1016/J.BIOMBIOE.2020.105614.

[23] D. L. 1986- Franco Jacome, “Caracterização físico-química das cinzas da palha de cana-de-açúcar através de análises térmicas simultâneas (STA),” 2014, Accessed: Aug. 17, 2021. [Online]. Available: http://repositorio.unicamp.br/jspui/handle/REPOSIP/265950.

[24] R. Manrique, D. Vásquez, F. Chejne, and A. Pinzón, “Energy analysis of a proposed hybrid solar–biomass coffee bean drying system,” *Energy*, vol. 202, pp. 1–8, 2020, doi: 10.1016/j.energy.2020.117720.

[25] M. Guerrero, M. P. Ruiz, M. U. Alzueta, R. Bilbao, and A. Millera, “Pyrolysis of eucalyptus at different heating rates: studies of char characterization and oxidative reactivity,” *J. Anal. Appl. Pyrolysis*, vol. 74, no. 1–2, pp. 307–314, Aug. 2005, doi: 10.1016/J.JAAP.2004.12.008.

[26] A. C. Gutierrez-Gomez, A. G. Gallego, R. Palacios-Bereche, J. Tofano de Campos Leite, and A. M. Pereira Neto, “Energy recovery potential from Brazilian municipal solid waste via combustion process based on its thermochemical characterization,” *J. Clean. Prod.*, vol. 293, p. 126145, Apr. 2021, doi: 10.1016/J.JCLEPRO.2021.126145.

[27] J. L. F. Alves *et al.*, “Lignocellulosic Residues from the Brazilian Juice Processing Industry as Novel Sustainable Sources for Bioenergy Production: Preliminary Assessment Using Physicochemical Characteristics,” *Artic. J. Braz. Chem. Soc*, vol. 31, no. 9, 2020, doi: 10.21577/0103-5053.20200094.

[28] S. Pan-In and N. Sukasem, “Methane production potential from anaerobic co-digestions of different animal dungs and sweet corn residuals,” *Energy Procedia*, vol. 138, pp. 943–948, 2017, doi: 10.1016/j.egypro.2017.10.062.

[29] M. Puig-Arnavat, J. C. Bruno, and A. Coronas, “Modified Thermodynamic Equilibrium Model for Biomass Gasification: A Study of the Influence of Operating Conditions,” *Energy \& Fuels*, vol. 26, no. 2, pp. 1385–1394, 2012, doi: 10.1021/ef2019462.

[30] P. A. Silva Ortiz, “Hierarquização exergética e ambiental de rotas de produção de bioetanol.,” Biblioteca Digital de Teses e Dissertações da Universidade de São Paulo, São Paulo, 2017.

[31] E. M. Medeiros *et al.*, “Preliminary assessment by the Virtual Sugarcane Biorefinary framework of syngas production and power generation from a first-generation sugacane plant lignocellulosic biomass.,” *5th Int. Conf. Eng. Waste Biomass Valoris.*, no. September 2015, 2014.

[32] V. Marcantonio, M. De Falco, M. Capocelli, E. Bocci, A. Colantoni, and M. Villarini, “Process analysis of hydrogen production from biomass gasification in fluidized bed reactor with different separation systems,” *Int. J. Hydrogen Energy*, vol. 44, no. 21, pp. 10350–10360, 2019, doi: https://doi.org/10.1016/j.ijhydene.2019.02.121.

[33] F. M. Cavalcanti, M. Schmal, R. Giudici, and R. M. Brito Alves, “A catalyst selection method for hydrogen production through Water-Gas Shift Reaction using artificial neural networks,” *J. Environ. Manage.*, vol. 237, pp. 585–594, May 2019, doi: 10.1016/J.JENVMAN.2019.02.092.

[34] F. Günther and S. Fritsch, “neuralnet: Training of Neural Networks,” *R J.*, vol. 2, no. 1, pp. 30–38, 2010, doi: 10.1109/SP.2010.25.

[35] G. Rothenberg, “Data mining in catalysis: Separating knowledge from garbage,” *Catal. Today*, vol. 137, no. 1, pp. 2–10, Aug. 2008, doi: 10.1016/J.CATTOD.2008.02.014.

[36] D. Flórez-Orrego and S. de Oliveira Junior, “On the efficiency, exergy costs and CO2 emission cost allocation for an integrated syngas and ammonia production plant,” *Energy*, vol. 117, pp. 341–360, 2016, doi: https://doi.org/10.1016/j.energy.2016.05.096.

[37] D. Flórez-Orrego, F. Nascimento Silva, and S. de Oliveira Junior, “Syngas production with thermo-chemically recuperated gas expansion systems: An exergy analysis and energy integration study,” *Energy*, vol. 178, pp. 293–308, Jul. 2019, doi: 10.1016/J.ENERGY.2019.04.147.

[38] M. Bagheri, R. Esfilar, M. Sina Golchi, and C. A. Kennedy, “Towards a circular economy: A comprehensive study of higher heat values and emission potential of various municipal solid wastes,” *Waste Manag.*, vol. 101, pp. 210–221, Jan. 2020, doi: 10.1016/J.WASMAN.2019.09.042.

[39] ASPENTECH, “Aspen Plus V8.8.” 2011.

[40] J. Szargut, D. R. Morris, and F. R. Steward, “Exergy analysis of thermal, chemical, and metallurgical processes,” 1987.

[41] S. A. Channiwala and P. P. Parikh, “A unified correlation for estimating HHV of solid, liquid and gaseous fuels,” *Fuel*, vol. 81, no. 8, pp. 1051–1063, 2002, doi: https://doi.org/10.1016/S0016-2361(01)00131-4.

[42] J. Parikh, S. A. Channiwala, and G. K. Ghosal, “A correlation for calculating HHV from proximate analysis of solid fuels,” *Fuel*, vol. 84, no. 5, pp. 487–494, 2005, doi: 10.1016/j.fuel.2004.10.010.

[43] A. C. Caetano de Souza, J. Luz-Silveira, and M. I. Sosa, “Physical-Chemical and Thermodynamic Analyses of Ethanol Steam Reforming for Hydrogen Production,” *J. Fuel Cell Sci. Technol.*, vol. 3, no. 3, pp. 346–350, Aug. 2006, doi: 10.1115/1.2217957.

https://doi.org/10.52202/069564-0150